Trees, Forests and People 26 (2026) 101367

Contents lists available at ScienceDirect

Trees, Forests and People

journal homepage: www.sciencedirect.com/journal/trees-forests-and-people

Conflict-driven rapid forest degradation in an urban riparian ecosystem: High-resolution satellite evidence from Sunut Reserved Forest, Sudan

Abdalrahman Ahmed [a,b,*], Abubakr Osman [a,c], Kornel Czimber [a]

[a] Institute of Geomatics and Civil Engineering, Faculty of Forestry, University of Sopron, Bajcsy-Zs 4, Sopron, 9400, Hungary
[b] Department of Forest and Environment, Faculty of Forest Sciences and Technology, University of Gezira, P.O. Box 20, Wad Madani, Sudan
[c] Department of Forest Management, Faculty of Forestry, University of Khartoum, Khartoum, 13314, Sudan

ARTICLE INFO

Keywords:
Land cover
Degradation
Forest
Urban
War

ABSTRACT

Armed conflict is increasingly recognized as a driver of rapid land degradation, particularly in regions where the breakdown of the governance accelerates unsustainable resource extraction. This study quantified conflict-associated forest degradation in the Sunut Reserved Forest, a riparian ecosystem in Khartoum, Sudan, following the escalation of armed conflict in 2023. Multi-temporal PlanetScope imagery from January 2023, 2024, 2025, and 2026 was analyzed to assess vegetation dynamics and land cover transitions. Vegetation dynamics were assessed using the Normalized Difference Vegetation Index (NDVI), and land use/land cover (LULC) classification was performed using an object-based Support Vector Machine (SVM) algorithm. A total of 260–272 stratified random samples per year were used, with 70% allocated for training and 30% for independent validation. The classification performance was evaluated using confusion matrix–based metrics, yielding overall accuracies ranging from 82.09% to 94.10% and Kappa coefficients between 0.64 and 0.88.

Forest cover declined from 105.34 ha (58.23%) in 2023 to 20.19 ha (11.16%) in 2026, representing 80.83% reduction over three years. Annual forest loss accelerated from -12.66 ha·yr^{-1} (2023–2024) to -36.25 ha·yr^{-1} (2024–2026), and sharply increased to -66.66 ha·yr^{-1} ($\approx -76.75\%$·yr^{-1}) between 2025 and 2026, indicating a non-linear degradation trajectory. NDVI correlations weakened substantially over time ($\tau = 0.69$ for 2023–2024; $\tau = 0.20$ for 2024–2026; $p < 0.001$), reflecting the structural collapse of canopy integrity. Analysis of long-term climate data (2015–2025) showed no significant rainfall or temperature anomalies, indicating that climatic variability is unlikely to explain the observed vegetation decline in the area. The classification accuracy exceeded 88% ($\kappa > 0.80$), and the uncertainty estimates were considerably smaller than the magnitude of the detected changes. Spatial evidence confirms that direct deforestation activities, rather than climatic stress, are the primary drivers.

The near-complete removal of riparian forest cover implies severe degradation of hydrological regulation, soil stability, and biodiversity in urban floodplain settings. These findings demonstrate how conflict can trigger abrupt land system transitions and underscore the need for conflict-resilient land governance, rapid restoration interventions, and satellite-based monitoring frameworks to prevent long-term degradation and loss of ecosystem services.

1. Introduction

Forests are critical components of terrestrial systems, providing climate regulation, biodiversity support, hydrological stabilization, carbon sequestration, and socio-economic services (Foley et al., 2005; Krieger, 2001; Mishkin and Navarrete Pacheco, 2022). Changes in forest cover, whether through deforestation, degradation, or fragmentation, directly influence ecosystem service provision and land system resilience (Balthazar et al., 2015; Hosonuma et al., 2012). Globally, forest cover change (FCC) reflects complex interactions among biophysical conditions, demographic pressures, governance structures, economic incentives and policy interventions (Geist and Lambin, 2002; Lambin et al., 2001; Vanonckelen and Van Rompaey, 2015). While afforestation and natural regrowth have occurred in certain regions (Baumann et al., 2011; Winkler et al., 2021), forest loss remains dominant across much of the Global South, driven by agricultural expansion,

* Corresponding author.
E-mail address: ix3mzk@uni-sopron.hu (A. Ahmed).

https://doi.org/10.1016/j.tfp.2026.101367

Available online 23 June 2026

fuelwood extraction, urbanization, and weak institutional enforcement (Davis et al., 2020; Rudel et al., 2009).

In fragile and conflict-affected states, deforestation dynamics often intensify owing to governance breakdown, displacement pressures, and informal resource extraction (Baumann and Kuemmerle, 2016; Gaynor et al., 2016). Armed conflict can disrupt environmental regulation, weaken protected area enforcement, and increase dependence on forest resources for fuel and shelter (Meaza et al., 2024). Empirical evidence from conflict-affected regions, including the Democratic Republic of Congo, Colombia, and parts of the Sahel, demonstrates that forest ecosystems frequently experience accelerated degradation during and after periods of instability (Clerici et al., 2020; Ordway, 2015). However, quantitative assessments of conflict-driven forest loss remain limited in Sudan, despite its documented environmental vulnerability.

Sudan is characterized by diverse but ecologically fragile ecosystems, particularly in arid and semi-arid zones that are highly sensitive to rainfall variability and anthropogenic pressure (Ahmed et al., 2018; Yousif et al., 2018). Historically, recurrent droughts, land degradation, overgrazing, and unsustainable wood extraction have contributed to forest decline (K. T. Osman, 2014; Sulieman, 2018). In Darfur and other regions, environmental stress is closely intertwined with socio-political instability, displacement, and resource competition (Kranz et al., 2015; Sulieman and Ahmed, 2013). However, recent climatic analyses suggest partial vegetation greening trends in parts of western Sudan due to increased precipitation and land abandonment (Ahmed, Rotich, and Czimber, 2025), highlighting the need to distinguish climatic recovery from anthropogenic forest removal in this region.

Khartoum State hosts one of Sudan's most significant urban forest ecosystems the Al-Sunut Forest Reserve. The riparian forest along the White Nile has recreational, ecological, and economic value (Yusif et al., 2023, 2024). Beyond its social importance, the Sunut Forest functions as a hydrological buffer, mitigating flood risks and stabilizing riverbank soils. Participatory forest management initiatives in Khartoum State have previously emphasized conservation and community engagement as essential components of sustainable forest governance (Elzubair et al., 2024). However, the armed conflict that began on April 15, 2023, severely disrupted institutional structures, public services, and regulatory oversight (Huang et al., 2023; Mahgoub et al., 2024). Under such conditions, increased reliance on fuelwood and charcoal production can intensify forest exploitation.

Prior to the 2023 conflict, available evidence suggested that the Sunut Reserved Forest remained relatively intact despite ongoing urban pressures. Previous studies have described forests as well-maintained riparian ecosystems that provide ecological, recreational, and educational services in Khartoum (Yusif et al., 2023, 2024). Management by the Forest National Corporation (FNC) and local conservation initiatives contributed to maintaining forest structure, with no documented evidence of rapid or large-scale deforestation comparable to that observed in the post-2023 period. Although urban expansion and development pressures pose intermittent threats (M. M. Osman and Sevinc, 2019), they do not result in abrupt canopy loss or landscape-scale conversion. In contrast, the changes observed in this study between 2023 and 2026 are spatially extensive and temporally abrupt, indicating a clear shift from relatively stable conditions to rapid mangrove forest degradation. This distinction supports the interpretation that the observed forest loss is primarily associated with post-conflict dynamics rather than a pre-existing long-term decline in forest cover.

While the humanitarian and economic impacts of the Sudan conflict have been widely documented, systematic quantification of the associated land degradation particularly within urban protected forests remains scarce. The intersection of conflict, rapid urban environmental degradation, and ecosystem service loss represents a critical research gap that requires urgent attention from researchers. High-resolution remote sensing offers a powerful means of monitoring forest dynamics in inaccessible or insecure regions, enabling the timely detection of abrupt land system transitions (Guo et al., 2022; Townshend et al., 2012).

National and international attention to the degradation of the Sunut Reserved Forest increased in 2025, as reports documented extensive tree loss within the reserve. During the conflict, fuel shortages, disruption of energy supplies, and the collapse of basic services increased the reliance on firewood and charcoal as alternative energy sources in Khartoum (Basheer and Elagib, 2024; CEOBS, 2025). Several organizations and media outlets, including the Conflict and Environment Observatory (CEOBS), UNEP, France 24 and TRT World, reported tree cutting and habitat degradation within the Sunut Forest linked to conflict-related resource extraction and weakened environmental governance (France 24, 2026; UNEP, 2025). Public concern peaked in early 2026, following the widespread circulation of field observations documenting severe forest destruction. Despite these reports, quantitative assessments of the extent and rate of forest loss are lacking.

Land Use and Land Cover Change (LULCC) analysis, supported by remote sensing (RS) and geographic information systems (GIS), has become central to understanding degradation processes and guiding sustainable land management (Chaves et al., 2020; Nedd et al., 2021). Accurate LULCC information informs assessments of soil erosion, hydrological alteration, biodiversity loss, ecosystem service decline, and land surface temperature changes (Biswas and Islam, 2025; Khan and Chen, 2025; Mir et al., 2025). In semi-arid environments, distinguishing between drought-driven vegetation fluctuations and direct deforestation is particularly important for interpreting the degradation pathways.

Against this backdrop, the present study investigated forest cover dynamics in the Sunut Reserved Forest between 2023 and 2026 using high-resolution satellite imagery and quantitative change analysis. Specifically, we aimed to quantify the magnitude and rate of forest cover loss following the escalation of armed conflict in 2023, characterize the temporal trajectory and acceleration of land cover transitions, and evaluate the potential implications of forest depletion for urban ecosystem resilience in a semi-arid floodplain context.

By providing empirical evidence of rapid conflict-associated deforestation within an urban riparian ecosystem, this study contributes to a broader understanding of land degradation processes under socio-political instability. This further demonstrates the utility of high-resolution satellite monitoring for detecting abrupt ecosystem transitions in fragile regions and supports the integration of remote sensing into conflict-sensitive environmental governance.

2. Data and methods

2.1. Study area

The Sunut Reserved Forest is located in Khartoum State, central Sudan, near the urban core of Khartoum. The reserve lies between approximately 15°35′–15°36′ N latitude and 32°30′–32°31′ E longitude, along the western bank of the White Nile near its confluence with the Blue Nile (Fig. 1). This position within the Nile floodplain historically provided relatively fertile alluvial soils and shallow groundwater availability, enabling the development of a riparian gallery forest ecosystem within the otherwise semi-arid landscape of the Nile.

Khartoum has a hot semi-arid climate (BSh, Köppen classification) characterized by a mean annual rainfall of approximately 150–250 mm, concentrated between July and September, followed by a prolonged dry season. Summer temperatures frequently exceed 40–45 °C, and natural vegetation outside riverine corridors is generally sparse and drought-adapted (Yusif et al., 2023). In this climatic setting, the river-fed woodlands of the Sunut Forest represent a rare and ecologically significant green refuge within an expanding metropolitan area.

The study area covered approximately 180.90 ha. Prior to large-scale degradation, the forest was dominated by dense stands of *Acacia nilotica* (locally known as "Sunut"), *Khaya senegalensis* (African mahogany) and other indigenous species. The structure included mixed woodlands,

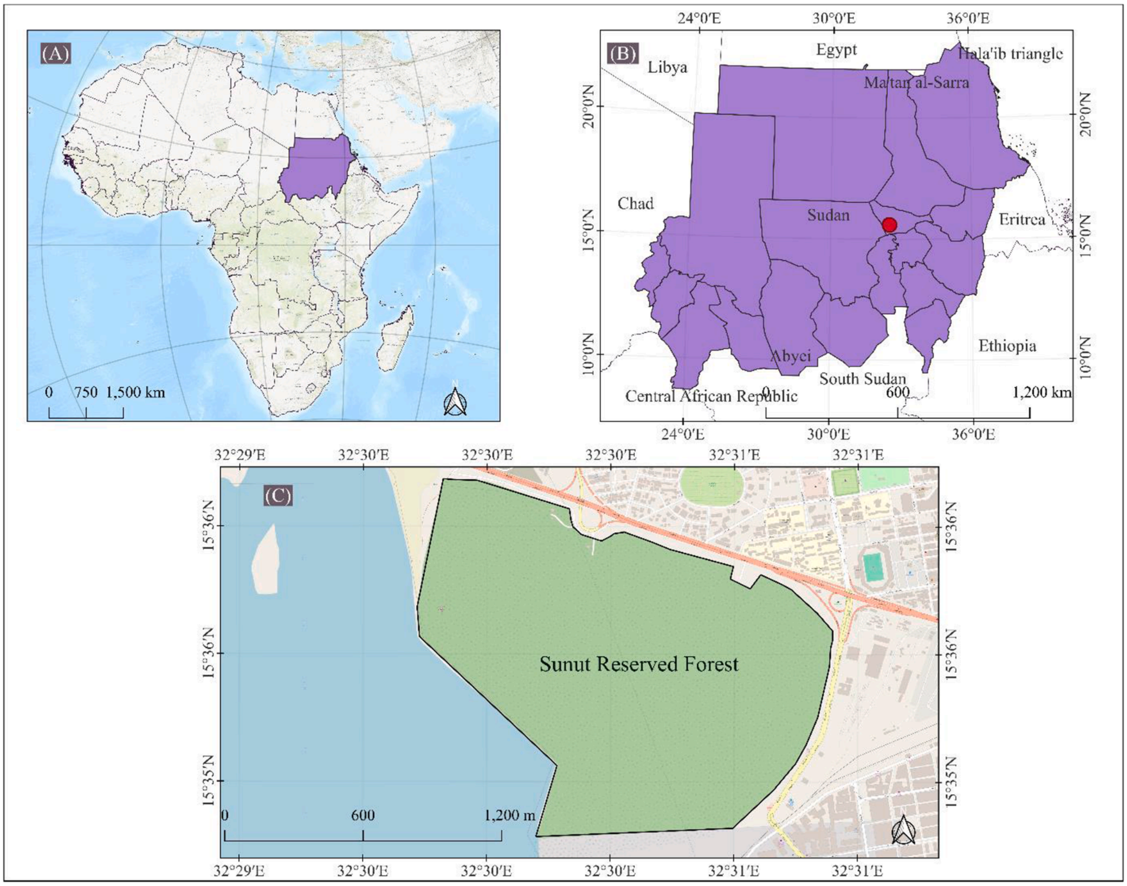

Fig. 1. Illustrates (A) the location of Sudan within Africa, (B) the location of the Sunut Reserved Forest within Sudan, and (C) the spatial extent of the study area along the White Nile.

wetlands, and grass clearings that supported high habitat heterogeneity. The reserve was legally designated as a protected forest and bird sanctuary by Sudanese forestry legislation. Ecological surveys have documented >100 bird species, including migratory waterfowl and passerines, as well as reptiles and small mammals that are typical of riparian ecosystems (Salah et al., 2013).

Beyond biodiversity value, the Sunut Forest provides significant ecosystem services, including riparian stabilization and flood buffering along the White Nile, microclimate regulation in a densely urbanized area, carbon storage and biomass production, and recreation, environmental education, and scientific research (Yusif et al., 2024). Economic valuation studies have highlighted the importance of the park as one of the few natural recreational spaces available to the residents of Khartoum (Yusif et al., 2023). Its proximity to the capital make it both socially valuable and environmentally vulnerable.

2.1.1. Pre-conflict management context

Before 2023, the forest was managed by the Forest National Corporation (FNC) of Sudan in coordination with local conservation actors. Although urban expansion and infrastructure pressures pose intermittent threats, the reserve has remained relatively intact due to institutional oversight and public advocacy. Participatory forest management initiatives in Khartoum State have emphasized conservation and sustainable use practices (Elzubair et al., 2024).

2.1.2. Conflict context and environmental vulnerability

On April, 15, 2023, armed conflict escalated in Khartoum, resulting in widespread institutional collapse, infrastructure damage, and a humanitarian crisis (Mahgoub et al., 2024; Zou et al., 2023). As governance structures weakened and fuel supplies became scarce, the reliance on fuelwood and charcoal increased sharply. In conflict-affected settings, forests often become accessible resource reservoirs when enforcement mechanisms fail (Baumann and Kuemmerle, 2016; Meaza et al., 2024).

Although the Sunut Forest was not initially a direct combat target, its location near industrial and strategic zones exposed it to indirect pressure. Restricted access prevents active monitoring and enforcement by forestry authorities (CEOBS, 2025b). Reports indicated tree cutting for fuelwood, charcoal production, and potentially temporary fortifications during the conflict period. By 2026, camera documentation revealed extensive canopy removal and fragmentation across the reserve (Fig. 2).

The Sunut Reserved Forest thus provides a critical case study of how urban protected forests in semi-arid regions can experience rapid land degradation under the conditions of governance breakdown. Its location within the Nile floodplain further amplifies the ecological significance of the observed deforestation, given the role of riparian vegetation in hydrological regulation and in flood mitigation.

2.2. Satellite data acquisition and preprocessing

2.2.1. Image selection

To quantify forest degradation dynamics in the Sunut Reserved Forest, high-resolution multispectral imagery from the PlanetScope constellation (Planet Labs Inc., USA) https://www.planet.com/ was used. PlanetScope provides near-daily coverage at approximately 3 m spatial resolution with four spectral bands (blue, green, red, near-infrared), enabling fine-scale monitoring of small protected areas (Atwal et al., 2026). Four cloud-free PlanetScope Analytic Ortho Scene images were acquired in February 2023, 2024, 2025, and 2026 (Table 1). The February 2023 image was acquired prior to the outbreak

Fig. 2. Photos from the study area illustrating the remainign scrubs in the study area (February 2026).

Table 1
Summary of utilized images.

Acquisition Date	Data Source	Resolution (m)	Bands	Parameter of Interest
2023–01–20	PlanetScope Scene	3	RGB + NIR	Land use/Land cover
2024–01–20	PlanetScope Scene	3	RGB + NIR	Land use/Land cover
2025–01–20	PlanetScope Scene	3	RGB + NIR	Land use/Land cover
2026–01–20	PlanetScope Scene	3	RGB + NIR	Land use/Land cover

of armed conflict in Sudan on April 15, 2023, and was therefore used as the pre-conflict baseline. The 2024, 2025, and 2026 images represent the early, intermediate, and late phases of the conflict, respectively. To minimize the influence of seasonal variability and hydrological fluctuations associated with the Nile flood regime, all images were acquired on the same date (January 20) for each study year (2023, 2024, 2025, and 2026). January corresponds to the dry season in Khartoum, when vegetation phenology is relatively stable and river levels are low. This temporal consistency ensures that observed differences in the Normalized Difference Vegetation Index (NDVI) and land cover are primarily attributable to actual vegetation change rather than seasonal or hydrological effects (Ahmed, Rotich, Kipkulei, et al., 2025). Controlling for seasonality is critical in semi-arid systems, where NDVI variability can reflect rainfall anomalies rather than land-cover change.

All images were radiometrically calibrated and provided as surface reflectance products. Cloud and cloud-shadows were masked, and all datasets were reprojected to UTM Zone 36 N (WGS84). Although surface reflectance products reduce atmospheric effects, minor residual atmospheric variability may remain. Preprocessing was conducted in QGIS (v3.34) using the Orfeo Toolbox (OTB) modules. The geometric consistency was verified using stable landscape features (e.g., river channels and road networks). Accurate co-registration is essential for multi-temporal change detection to avoid artificial pixel-level differences (Han and Oh, 2018).

2.3. Vegetation condition assessment

Vegetation conditions were quantified using the Normalized Difference Vegetation Index (NDVI), Eq. (1) (Tucker, 1979).

$$NDVI = \frac{NIR - Red}{NIR + Red} \tag{1}$$

where *NIR* and *Red* represent the near-infrared and red reflectance, respectively. The NDVI ranges from -1 to $+1$, with higher values indicating dense, photosynthetically active vegetation and lower values indicating sparse or non-vegetated surfaces. NDVI has been widely validated for assessing vegetation vigor and biomass, particularly in semi-arid systems. Pixel-wise NDVI maps were generated for each year (2023, 2024, 2025, and 2026).

2.3.1. Statistical data analysis

All statistical analyses were conducted to quantify the temporal vegetation dynamics, assess interannual variability, and evaluate the significance of the observed changes in land cover and vegetation conditions. NDVI was computed from PlanetScope imagery for each study year (2023–2026). NDVI values were analyzed at the pixel level to characterize the spatial and temporal patterns of vegetation conditions.

To evaluate the consistency of NDVI patterns across years, Kendall's rank correlation coefficient (τ) was applied to the pairwise combinations of annual NDVI datasets. This non-parametric statistic was selected because of its robustness to non-normal distributions and its suitability for detecting monotonic relationships in spatial data.

Differences in NDVI distributions among years were assessed using the Kruskal–Wallis test, a non-parametric alternative to one-way ANOVA. This test was used to determine whether statistically significant differences existed in vegetation conditions across the four study years. Where significant differences were detected, post hoc pairwise comparisons were performed using the Wilcoxon rank-sum test, with the Benjamini–Hochberg correction applied to control for multiple testing and reduce the risk of Type I error.

Land use/land cover (LULC) changes were quantified using a combination of area-based change detection and intensity analyses. Absolute changes (ha), proportional changes (%), and annualized rates of change ($ha \cdot yr^{-1}$ and $\% \cdot yr^{-1}$) were calculated for the forest and non-forest classes. Interval-specific change intensity was computed to evaluate the rate and acceleration of land transformation between consecutive periods of time. All statistical analyses were performed using R statistical software (version 4.2), and spatial processing and classification were conducted usig QGIS (v3.34) and the Orfeo Toolbox (OTB).

Climate data, including mean annual rainfall and mean air temperature, were obtained from the Khartoum meteorological station for the period of 2015–2025. Data were analyzed and visualized using R statistical software.

2.4. LULC classification

2.4.1. Object-based image analysis (OBIA)

Given the high spatial resolution (3 m), an object-based image analysis (OBIA) approach (Ming et al., 2015), was adopted to reduce the noise typical of pixel-based classification. Image segmentation was performed using the Mean Shift algorithm implemented in Orfeo Toolbox (OTB) version 8.1.2. Mean Shift clustering groups pixels according to spectral similarity and spatial proximity without requiring a priori specification of cluster numbers (Cechim Junior et al., 2023; Zheng et al., 2009). Segmentation parameters were selected using the default OTB settings, which provided a satisfactory balance between over- and under-segmentation for the relatively simple binary classification scheme adopted in this study. The parameters included a spatial radius of 5 pixels, range radius of 15, and maximum number of 100 iterations.

2.4.2. Supervised classification

A binary LULC scheme was adopted consisting of (1) forest cover and (2) non-forest. This simplified classification was appropriate given the study's primary objective of quantifying deforestation, the limited feasibility of field data collection under conflict conditions, and the clear spectral separability between closed-canopy vegetation and non-vegetated or sparsely vegetated surfaces in the study area. Training samples were generated using a stratified random sampling approach to ensure an adequate spatial representation of both classes across the study area. The total number of samples used for each year was 2023 = 262 samples, 2024 = 270 samples, 2025 = 272 samples, and 2026 = 260 samples. For each year, the samples were randomly divided into 70% for training and 30% for independent validation, improving model generalization and reducing overfitting relative to equal split approaches. The sample size was selected to ensure adequate representation of both land-cover classes across the study area while maintaining a balanced training and validation dataset. Although a formal probabilistic sample size calculation (e.g., Cochran's formula) was not applied, the number of samples used exceeds commonly recommended minimum thresholds for binary land-cover classification and accuracy assessment in medium to high-resolution remote sensing studies (Congalton and Green, 2009). Classification was performed using a Support Vector Machine (SVM) classifier implemented in the OTB TrainVectorClassifier module. The classifier employed a Radial Basis Function (RBF) kernel, which is widely used in remote sensing applications because of its ability to model non-linear class boundaries. The penalty parameter (C) and kernel settings were retained at the default OTB configuration, which provided stable classification performance across all study years.

2.4.3. Accuracy assessment

The classification performance was evaluated using a confusion matrix–based accuracy assessment, which is widely recommended for validating thematic classification outputs (Congalton and Green, 2009; Gashaw et al., 2018). The following accuracy metrics were computed.

1- User's Accuracy (UA)

User accuracy represents the probability that a pixel classified into a given category actually belongs to that category on the ground (i.e., the reliability of the map), as shown in Eq. (2).

$$UA = \frac{Correctly\ classified\ pixels}{Column\ total} \times 100 \tag{2}$$

2- Producer's accuracy (PA)

The producer's accuracy indicates the probability that a reference pixel is correctly classified (i.e., omission error), as shown in Eq. (3).

$$PA = \frac{Correctly\ classified\ pixels}{Row\ total} \times 100 \tag{3}$$

3- Overall accuracy (OA)

Overall Accuracy measures the proportion of correctly classified pixels relative to the total number of validation samples, as shown in Eq. (4).

$$OA = \frac{Total\ number\ of\ correctly\ classified\ pixels}{Total\ number\ of\ pixels} \times 100 \tag{4}$$

4- Kappa Coefficient (κ)

The Kappa coefficient evaluates the agreement between the classification and reference data while accounting for agreement occurring by chance. The K value was calculated using Eq. (5), as follows:

$$K = \frac{OA - EA}{1 - EA} \tag{5}$$

where K is the Kappa coefficient, OA is the proportion of actual agreement between raters, and EA is the proportion of agreement expected by chance.

2.4.4. Reference data and validation strategy

Validation data were derived primarily from independent high-resolution imagery available in Google Earth Pro, supplemented by expert visual interpretation and local knowledge of the study area. Google Earth imagery served as the principal reference source and ensured independence from the PlanetScope data used for classification, thereby minimizing potential autocorrelation bias. PlanetScope imagery was used only as ancillary support for visual interpretation where temporal coverage of reference imagery was limited, particularly for 2026. The potential uncertainty associated with this approach is acknowledged in the limitations section of this paper. Validation samples were generated using a stratified random sampling approach, ensuring a balanced representation of both forest and non-forest classes across the study area. The accuracy assessment was conducted at the pixel level, resulting in larger sample counts in the confusion matrices than in the initial number of sampled locations. The use of independent reference data and a stratified validation design enhanced the reliability and robustness of classification results. All PlanetScope imagery was accessed under research and educational licensing agreements and processed according to the Planet Labs data policies.

2.5. Change detection and intensity analysis

Forest-to-non-forest transitions were quantified by calculating absolute area changes (ha), computing proportional changes (%), estimating annualized change rates ($ha \cdot yr^{-1}$), and assessing relative change intensity ($\% \cdot yr^{-1}$). The interval-specific change intensity was derived using Eq. (6), as follows:

$$Rate = \frac{A_{t2} - A_{t1}}{\Delta t} \tag{6}$$

where A_{t1} and A_{t2} represent forest areas at times 1 and 2 respectively. This framework enables the diagnosis of temporal acceleration and distinguishes gradual degradation from abrupt structural collapses.

3. Results

3.1. Classification accuracy assessment

The classification accuracy assessment indicated that the SVM model consistently achieved a strong performance in discriminating between forest and non-forest classes across all study years (Tables 2–5). The overall classification accuracy ranged from 82.09% to 94.10%, demonstrating a high level of agreement between the classified outputs and reference data. The highest accuracy was obtained in 2026 (94.10%), while the lowest was observed in 2025 (82.09%), although both were within the acceptable thresholds for LULC classification in heterogeneous landscapes.

The Kappa coefficient values ranged from 0.64 to 0.88, indicating substantial to near-perfect agreement beyond chance. Specifically, the κ values for 2023 (0.70) and 2024 (0.73) reflect substantial agreement, while 2026 (0.88) indicates near-perfect classification performance. The relatively low κ value in 2025 (0.64) suggests moderate classification uncertainty during that year, potentially reflecting transitional landscape conditions and increased heterogeneity.

Class-level accuracies further confirmed the robustness of the classification, with the producer's accuracy exceeding 80% for all classes and years, indicating a low omission error and strong ability of the classifier to correctly identify reference land-cover types. The user's accuracy was also consistently above 80%, reflecting a low commission error and high reliability of the mapped classes. For the forest class, PA ranged from 80.66% (2023) to 97.46% (2026), whereas UA ranged from 82.60% to 89.58%, indicating strong detection of forest pixels and minimal misclassification. The non-forest class exhibited similarly high performance, with PA values between 80.37% and 91.30% and UA values between 83.64% and 98.16%.

Table 2
Confusion matrix for the 2023 LULC classification showing pixel-level validation results, including Producer's Accuracy, User's Accuracy, Overall Accuracy, and Kappa coefficient.

	Reference Data			
Classified Data	Forest	Non-Forest	Total	UA
Forest	133	20	153	86.92
Non-Forest	51	283	334	84.73
Total	184	303	487	
PA	80.66	89.85		

Overall accuracy 85.66; Kappa Coefficient = 0.70.

Table 3
Confusion matrix for the 2024 LULC classification showing pixel-level validation results, including Producer's Accuracy, User's Accuracy, Overall Accuracy, and Kappa coefficient.

	Reference Data			
Classified Data	Forest	Non-Forest	Total	UA
Forest	141	22	163	82.60
Non-Forest	43	281	324	83.64
Total	184	303	487	
PA	86.50	86.73		

Overall accuracy 86.62; Kappa Coefficient = 0.73.

Table 4
Confusion matrix for the 2025 LULC classification showing pixel-level validation results, including Producer's Accuracy, User's Accuracy, Overall Accuracy, and Kappa coefficient.

	Reference Data			
Classified Data	Forest	Non-Forest	Total	UA
Forest	131	32	163	84.57
Non-Forest	53	271	324	88.43
Total	184	303	487	
PA	82.52	82.60		

Overall accuracy 82.09; Kappa Coefficient = 0.64.

Table 5
Confusion matrix for the 2026 LULC classification showing pixel-level validation results, including Producer's Accuracy, User's Accuracy, Overall Accuracy, and Kappa coefficient.

	Reference Data			
Classified Data	Forest	Non-Forest	Total	UA
Forest	129	15	144	89.58
Non-Forest	5	266	271	98.16
Total	134	281	415	
PA	97.46	91.30		

Overall accuracy 94.10; Kappa Coefficient = 0.88.
Note: PA – producer accuracy, UA – user accuracy.

Overall, the balanced and consistently high PA and UA values across both classes suggest no systematic bias toward over or under-classification of forest cover, which is critical for reliable deforestation assessment.

3.2. LULC transition

The LULC dynamics (Table 6) and (Fig. 3 Aand B) within the Sunut Reserved Forest for the years 2023, 2024, and 2026 reveal a pronounced decline in forested land and a corresponding expansion of non-forest areas, as spatially illustrated in (Fig. 4).

Forest Cover exhibited a substantial and continuous decrease throughout the study period. In 2023, forested areas occupied 105.34 ha, representing 58.23% of the Sunut Reserved Forest. By 2024, this decreased to 92.68 ha (51.23%), marking a loss of 12.66 ha in a single year. The most dramatic change occurred by 2026, when forest cover declined sharply to 20.19 ha, accounting for only 11.16% of the total area. This represents an overall forest loss of 85.15 ha between 2023 and 2026 corresponding to an 80.83% reduction in forested land within three years.

Complementing the decline in forest cover, non-forest areas expanded significantly. In 2023, non-forest land covered 75.56 ha (41.77%), and by 2024, it increased to 88.22 ha (48.77%), reflecting a gain of 12.66 ha. The most extensive expansion occurred by 2026, when the non-forest area reached 160.71 ha, occupying 88.84% of the Sunut Reserved Forest.

This indicates a total gain of 85.15 ha in non-forest land between 2023 and 2026, mirroring the forest loss over the same period.

The LULC changes reflect a clear and accelerating shift from forest to non-forest conditions, with the forested area shrinking from a dominant land cover class in 2023 to a minor and highly fragmented landscape by 2026. The major transition between 2025 and 2026 where forest cover dropped by 66.66 ha is indicative of rapid degradation processes and likely corresponds to extensive disturbance pressures within this period.

Table 6
LULC area statistics of Sunut reserved forest.

LULC Type	2023		2024		2025		2026	
	(ha)	%	(ha)	%	(ha)	%	(ha)	%
Forest Cover	105.34	58.23	92.68	51.23	86.85	48.01	20.19	11.16
Non-Forest	75.56	41.77	88.22	48.77	94.05	51.99	160.71	88.84
Total	180.90	100	180.90	100	180.90	100.00	180.90	100

3.3. *Interval-specific change intensity*

Considering the intervals explicitly clarifies how rapidly the landscape transformed (Fig. 3, B and C). 2023–2024 ($\Delta t = 1$ yr). Forest loss: -12.66 ha·yr^{-1} ($\approx -12.0\%$·yr^{-1} relative to 2023 Forest). Non-forest gain: $+12.66$ ha·yr^{-1} ($\approx +16.8\%$·yr^{-1} relative to 2023 non-forest). 2024–2025 ($\Delta t = 1$ yr). Forest loss: -5.83 ha·yr^{-1} ($\approx -6.29\%$·yr^{-1} relative to 2024 Forest). Non-forest gain: $+5.83$ ha·yr^{-1} ($\approx +6.60\%$·yr^{-1} relative to 2024 Non-Forest). 2024–2026 ($\Delta t = 2$ yr). Forest loss accelerates to -36.25 ha·yr^{-1} ($\approx -39.1\%$·yr^{-1} relative to 2024 Forest), while Non-Forest gains $+36.25$ ha·yr^{-1} ($\approx +41.1\%$·yr^{-1} relative to 2024 Non-Forest). 2025–2026 ($\Delta t = 1$ yr). Forest loss: -66.66 ha·yr^{-1} ($\approx -76.75\%$.yr^{-1} relative to 2025 Forest). Non-forest gain: $+66.66$ ha·yr^{-1} ($\approx +70.87\%$·yr^{-1} relative to 2025 Non-forest). Net (2023–2026, $\Delta t = 3$ yr). The forest declined by -85.15 ha (from 105.34 to 20.19 ha), while the non-forest increased by $+85.15$ ha (from 75.56 to 160.71 ha).

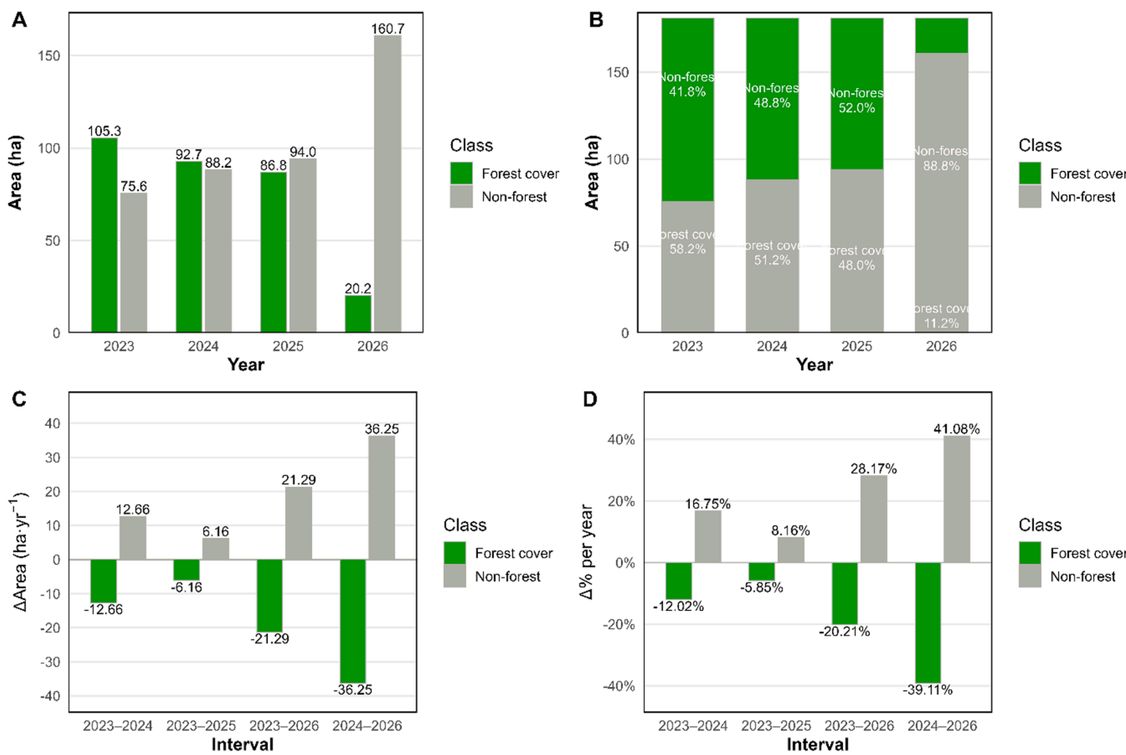

Fig. 3. shows (A) absolute area changes for forest versus non-forest across 2023, 2024, 2026, and (B) composition percent share per class per year, (C) change intensity ha.yr-1, and (D) change intensity percentage.year-1.

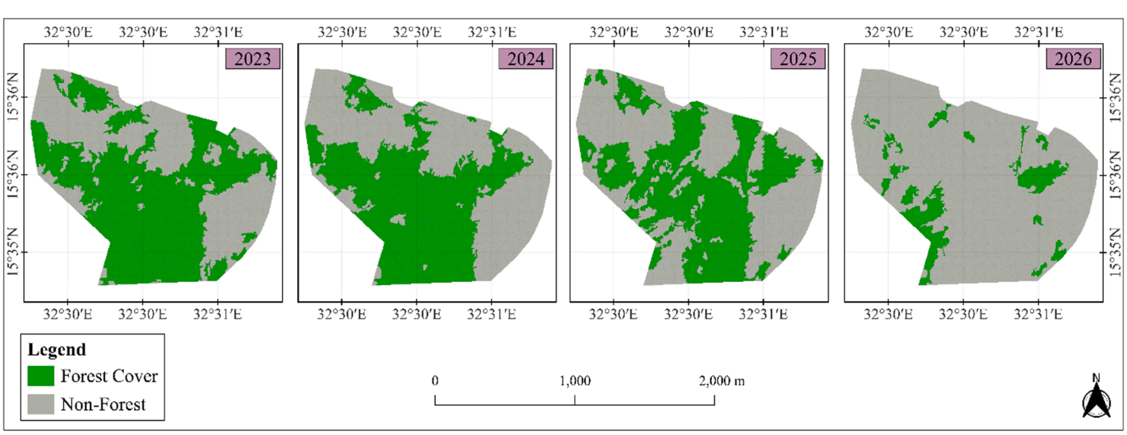

Fig. 4. The spatial distribution of LULC over 2023, 2024, and 2026.

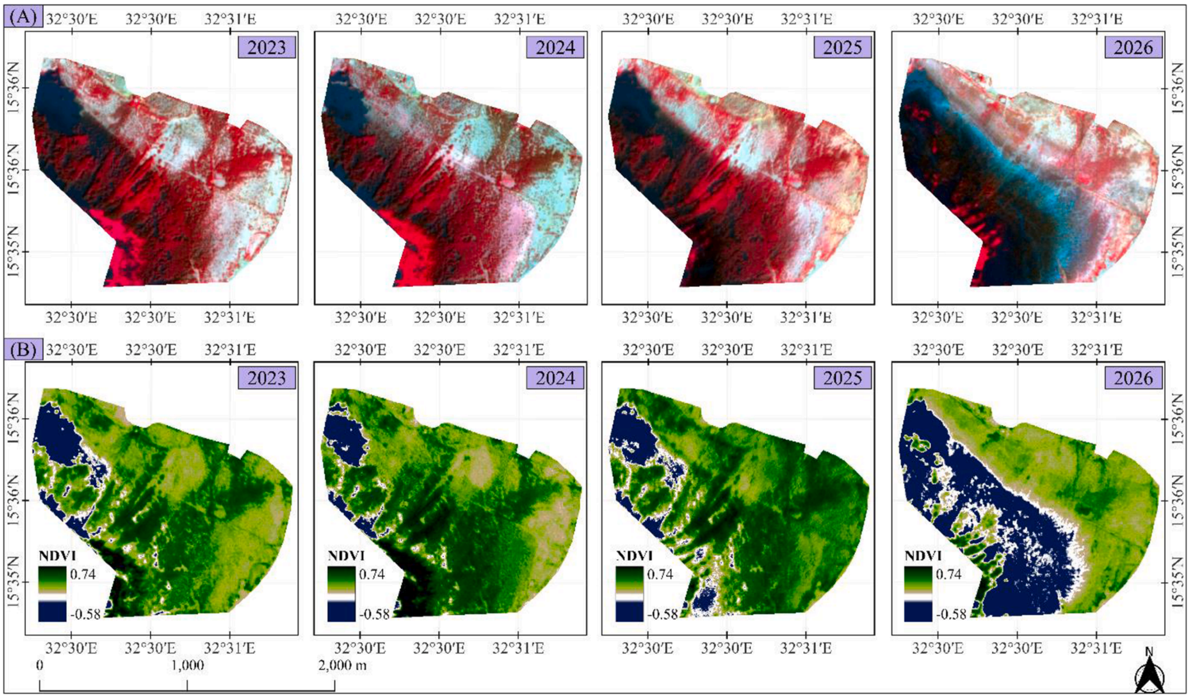

Fig. 5. Spatial distribution shows (A) PlnetScope false color composit (red, nir, and green).

3.4. NDVI trends

The spatial distribution of high-resolution imagery from PlanetScope, and the false-color composite of the PlanetScope data-sets show the removal of the forest canopy, which is particularly evident in 2026 (Fig. 5A). The NDVI analyzed maps of 2023, 2024, 2025 and 2026 (Fig. 5B) revealed an obvious decrease (deforestation) in the study area, especially in 2026.

3.4.1. Interannual NDVI consistency

Kendall's rank correlation analysis revealed varying degrees of consistency in the NDVI patterns across the study period (2023–2026) (Fig. 6). Strong positive correlations were observed between 2023 and 2024 ($\tau = 0.692$, $p < 0.0001$) and 2023 and 2025 ($\tau = 0.639$, $p < 0.0001$), indicating relatively stable spatial patterns of vegetation greenness during these intervals.

Similarly, the relationship between 2024 and 2025 remained relatively strong, further supporting the persistence of the vegetation structure prior to 2026. In contrast, correlations involving 2026 were markedly weaker, particularly for 2024–2026 ($\tau = 0.200$, $p < 0.0001$) and 2023–2026 ($\tau = 0.308$, $p < 0.0001$). This decline in correlation strength indicates a substantial reorganization of vegetation patterns in 2026 relative to previous years.

3.4.2. Differences in NDVI distributions

The Kruskal-Wallis test revealed statistically significant differences in NDVI distributions across all years ($\chi^2 = 891.17$, $p < 0.0001$), confirming the presence of interannual variability in vegetation conditions. Post-hoc pairwise comparisons using the Wilcoxon rank-sum test with Benjamini-Hochberg correction showed that all year-to-year differences were statistically significant (adjusted $p < 0.01$). However, the magnitude of these differences varied. The smallest difference occurred between 2024 and 2025 ($p = 0.0054$), indicating relatively similar vegetation conditions in these two years. In contrast, all comparisons involving 2026 showed extremely strong statistical significance ($p < 2 \times 10^{-16}$), highlighting pronounced deviations in vegetation

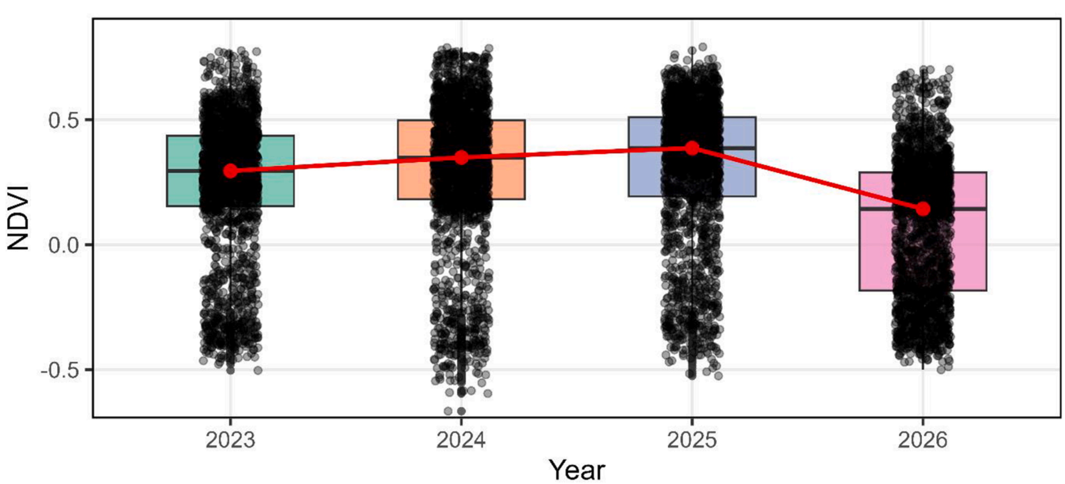

Fig. 6. NDVI variation accross 2023, 2024, and 2026.

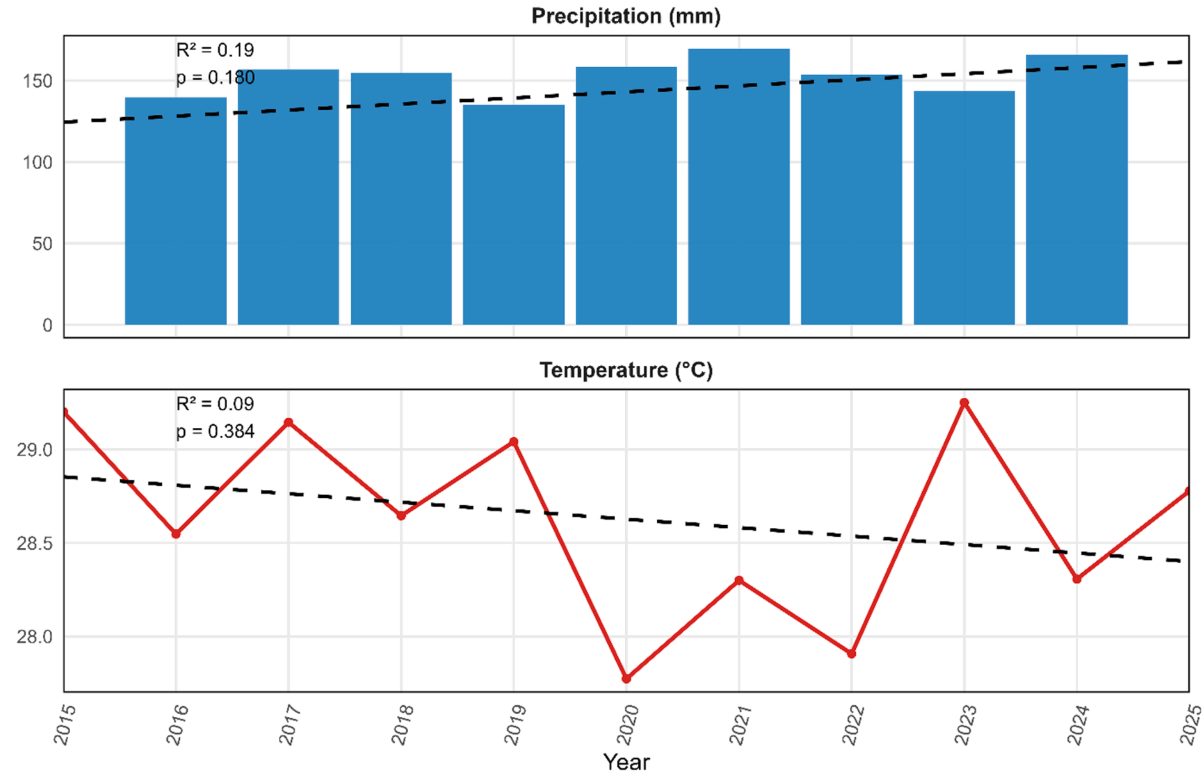

Fig. 7. Mean annual precipitation and temperature trends of the study area from 2015–2025.

structure during this year.

Taken together, these results indicate that NDVI patterns remained relatively stable from 2023 to 2025, with only moderate interannual variation. However, 2026 represents a clear breakpoint, characterized by reduced spatial correlation with previous years, strongly divergent NDVI distributions, and increased vegetation greenness heterogeneity in the region. These findings suggest that substantial vegetation change occurred between 2025 and 2026, marking a critical transition in the landscape.

3.5. Climate trend

Fig. 7 illustrates the mean annual precipitation and temperature trends for the period of 2015–2025. The results indicated a slight increasing trend in precipitation ($R^2 = 0.19$, $p = 0.180$) and a weak declining trend in temperature ($R^2 = 0.09$, $p = 0.384$), although neither trend was statistically significant.

4. Discussion

4.1. Mangnitude, accelaration, and direction of forest change

This study documented a rapid and structurally transformative deforestation event in the Sunut Reserved Forest, where forest cover declined substantially between 2023 and 2026. The change trajectory was temporally heterogeneous, with moderate loss between 2023 and 2025 followed by an abrupt collapse between 2025 and 2026. Such interval-specific acceleration is consistent with the analytical expectations of Intensity Analysis, which emphasizes the diagnosis of the size, rate, and category-level transitions of land-cover change through time (Aldwaik and Pontius, 2012). The observed shift from a forest-dominated landscape to a predominantly non-forest landscape reflects not gradual canopy thinning but extensive land-cover conversion. The reciprocal relationship between forest loss and non-forest expansion further indicates that the observed changes were driven primarily by direct deforestation rather than climatic variability, phenological fluctuations, or methodological artifacts. In Sudan, environmental degradation associated with conflict has been linked to illegal logging, charcoal production, and weakened environmental institutions (UNEP, 2007; Yasin et al., 2023). The acceleration detected between 2025 and 2026 is consistent with these documented mechanisms. Recent assessments of the environmental impacts of the Sudan conflict have reported extensive tree cutting for fuelwood and charcoal production in Khartoum State following institutional disruption and energy shortages (CEOBS, 2025b). Increased biomass extraction by households and displaced populations is therefore a plausible driver of the observed forest loss (Baumann and Kuemmerle, 2016; Gorsevski et al., 2012; Ordway, 2015). However, this explanation should be considered alongside other potential contributors, including informal settlement expansion, military activities, and localized infrastructure-related disturbances, which have also been documented in conflict-affected landscapes (Clerici et al., 2020; Eklund et al., 2017). Although direct field verification was not possible because of security constraints, the convergence of remote sensing evidence and established conflict-environment dynamics supports the interpretation that anthropogenic pressures intensified by the conflict were the primary drivers of deforestation.

The classification results further support this interpretation. Overall classification accuracy remained high throughout the study period (82.09–94.10%), indicating a robust discrimination between forest and non-forest classes. The relatively lower accuracy observed in 2025 ($OA = 82.09\%$; $\kappa = 0.64$) likely reflects the emergence of transitional landscape conditions preceding the large-scale forest loss detected in 2026. During this period, partial canopy thinning, fragmented vegetation patches, and mixed vegetation–bare soil surfaces increased spectral heterogeneity and reduced class separability, resulting in greater classification uncertainty. Such transitional conditions are commonly observed during the early stages of forest degradation, when canopy removal occurs incrementally before widespread conversion becomes evident. Despite this temporary reduction in classification performance, both overall accuracy and Kappa values remained within accepted thresholds for land-cover mapping, and the magnitude of the detected forest loss substantially exceeded the estimated classification uncertainty. Consequently, the observed deforestation trends are considered robust and unlikely to be an artifact of classification error.

4.2. Conflict-driven deforestation in Sudan and the regional context

Sudan has long experienced pressure on forest resources due to fuelwood demand, agricultural expansion, and weak enforcement capacities (Daur et al., 2016; FAO, 2020; Hassan et al., 2009; Musa et al., 2025). However, conflict introduces additional drivers, including the breakdown of environmental governance, expansion of informal charcoal economies, displacement-driven resource extraction, and reduced enforcement of protected areas. Studies in Darfur and South Sudan show that conflict zones often experience accelerated deforestation linked to the charcoal trade and survival strategies (Nicholson et al., 2018). Similar patterns have been observed in the Democratic Republic of the Congo and Colombia, where post-conflict transitions have paradoxically triggered forest loss due to governance vacuums (Clerici et al., 2020; Ordway, 2015; Van Uhm et al., 2022). The Sunut Forest trajectory mirrors these dynamics. The sharp inflection between 2025 and 2026 strongly suggests that deforestation intensified during periods of weakened regulatory oversight. The spatial coherence of canopy removal further indicates organized extraction rather than scattered subsistence harvesting in the region.

The absence of a significant decline in rainfall or an increase in temperature prior to 2026 suggests that climatic stress is unlikely to be the primary driver of the observed abrupt decline in vegetation. Instead, the relatively stable climatic conditions between 2015 and 2025 support the interpretation that the sharp reduction in NDVI and forest cover between 2025 and 2026 is primarily due to anthropogenic disturbances. Although climate does not appear to explain the magnitude or timing of change, its potential influence cannot be entirely excluded. Future studies integrating climate data with higher temporal resolution would further improve the attribution of vegetation dynamics.

4.3. Interpretation of NDVI dynamics

NDVI analysis provides strong statistical evidence of a non-linear temporal trajectory in vegetation dynamics, characterized by relative stability from 2023 to 2025 followed by a marked disruption in 2026. The high Kendall correlation coefficients between consecutive years prior to 2026 indicate that the spatial configuration of the vegetation remained largely consistent, suggesting limited structural disturbance during this period. In contrast, the sharp decline in correlation values involving 2026, combined with highly significant differences in NDVI distributions ($p < 2 \times 10^{-16}$), indicates a substantial reorganization of the vegetation patterns. Such divergence is unlikely to result solely from gradual ecological processes or seasonal variability, particularly given the use of temporally consistent imagery acquired during the same month each year.

The observed breakpoint between 2025 and 2026 is consistent with rapid land-cover transformation involving extensive canopy disturbance and fragmentation. However, NDVI primarily reflects vegetation greenness and canopy condition and therefore cannot independently distinguish between vegetation stress, partial canopy degradation, and complete forest removal. Consequently, reductions in NDVI should not automatically be interpreted as evidence of deforestation. In this study, NDVI dynamics were evaluated alongside object-based LULC classification and spatial change analysis. The concurrence of declining NDVI values, extensive forest-to-non-forest transitions, and increasing canopy fragmentation provides evidence that the observed changes reflect not only vegetation degradation but also the widespread physical removal of woody vegetation.

While NDVI variability can be influenced by climatic and hydrological factors, climate analysis revealed no significant trends in rainfall or temperature during 2015–2025, suggesting that climatic stress alone is unlikely to explain the abrupt decline observed in 2026. Furthermore, the magnitude and spatial coherence of the observed changes, together with the classification-based evidence of forest-cover conversion, indicate that anthropogenic disturbance was the dominant driver of vegetation change. In conflict-affected environments, such abrupt vegetation decline is commonly associated with increased resource extraction, land-use conversion, and the breakdown of environmental governance (Baumann et al., 2016; Baumann and Kuemmerle, 2016; Eklund et al., 2017; Nardi and Runnström, 2024). Accordingly, the term vegetation degradation is used in this study when referring to reductions in canopy greenness and vegetation condition inferred from NDVI, whereas deforestation refers specifically to the documented conversion of forest cover to non-forest land identified through the LULC classification. Overall, the combined NDVI and classification results indicate that 2026 represents a critical tipping point in ecosystem condition, reflecting both accelerated vegetation degradation and extensive deforestation within the study area.

4.4. Ecological consequences and ecosystem service lost

4.4.1. Flood regulation and hydrological stabilty

The Sunut Forest has historically functioned as a riparian buffer in the White Nile floodplain. Forest canopies reduce the impact of rainfall, increase infiltration, stabilize soils, and regulate surface runoff (Bruijnzeel, 2004; Ellison et al., 2017). The conversion of dense canopies to non-forest surfaces is likely to increase runoff velocity, reduce infiltration capacity, elevate sediment transport, and amplify flood risks. In urban floodplain environments such as Khartoum, the removal of riparian forest buffers can significantly increase exposure to seasonal flooding. The ecological services foregone by the 79% forest loss likely extend beyond the reserve boundaries.

4.4.2. Biodiversity implications

Previous ecological surveys have documented substantial biodiversity within the Sunut Forest, including >80 bird species and diverse arthropod communities (Eltayeb et al., 2012). Habitat fragmentation followed by near-total canopy removal suggests severe disruption of nesting habitats, migratory corridors, and trophic networks. Forest fragmentation theory demonstrates that a rapid reduction below critical area thresholds can lead to a disproportionate biodiversity collapse (Fahrig, 2003). The shift from a contiguous canopy to isolated remnants in 2026 likely exceeded the fragmentation thresholds necessary to maintain functional habitats.

4.4.3. Land degradation feedback

Deforestation in semi-arid regions can initiate degradation feedback loops, including soil compaction, reduced organic matter, and declining regeneration capacity. These processes are well documented across the Sahel and Nile Basin regions (Abdullahi et al., 2023; K. T. Osman, 2014; Reij et al., 2009). Without intervention, the regeneration of mature Acacia-dominated systems may tack decades.

4.4.4. Government breakdown as primerly mechanism

The temporal pattern of a moderate initial decline followed by an abrupt acceleration is consistent with governance disruption rather than a climatic anomaly. Climate-driven vegetation stress typically produces a gradual decline in NDVI, which is linked to rainfall variability (Nicholson et al., 2013). In contrast, the near-complete canopy removal observed in this study reflected direct biomass extraction. The environmental governance literature emphasizes that protected areas in conflict zones are highly vulnerable when enforcement capacity collapses (Duffy, 2006; Gaynor et al., 2016). The Sunut Reserved Forest exemplifies this vulnerability to climate change.

4.4.5. Limitations

Although field validation was not feasible because of the ongoing conflict, the magnitude of the detected forest loss substantially exceeded the estimated classification uncertainty, providing confidence in the overall change detection results. Validation was conducted primarily using independent high-resolution imagery available through Google Earth Pro; however, temporally exact reference imagery was not available for all dates, particularly for 2026. Consequently, some uncertainty may exist in the validation of the most recent classification. While efforts were made to minimize potential autocorrelation bias through the use of independent reference data, the limited temporal availability of very high-resolution imagery remains a constraint in conflict-affected environments.

The stratified random sampling design ensured balanced representation of forest and non-forest classes across the study area. However, a formal probabilistic sample size determination (e.g., Cochran's formula) was not applied. Although the number of samples used exceeded commonly recommended thresholds for binary land-cover classification and yielded satisfactory classification accuracies, future studies should evaluate optimal sample sizes under defined confidence levels and margins of error to further strengthen statistical rigor.

In addition to climatic variability, hydrological conditions may influence vegetation dynamics in riparian ecosystems. As continuous records of White Nile discharge, groundwater levels, and floodplain hydrology were not available for the study period, the influence of hydrological variability could not be explicitly evaluated. Consequently, the relative contributions of hydrological and anthropogenic drivers to vegetation change cannot be fully determined. Future research should integrate Sentinel-2 time series to capture intra-annual dynamics, apply landscape metrics (e.g., edge density, patch cohesion, and fragmentation indices), quantify aboveground biomass loss using radar or LiDAR data, incorporate hydrological monitoring, and assess post-conflict regeneration trajectories. Continuous NDVI monitoring has proven to be effective for detecting vegetation decline and recovery across African ecosystems (Pettorelli et al., 2005; Venter et al., 2020).

4.4.6. Policy and management implementation

The findings carry urgent implications for post-conflict recovery in Sudan including:

- Immediate reforestation using native species (e.g., *Acacia nilotica*).
- Establishment of conflict-resilient environmental governance frameworks.
- Institutionalization of satellite-based forest monitoring.
- Control of illegal logging and charcoal production.
- Integration of forest restoration into urban flood risk management strategies.

Environmental protection must be embedded within national stabilization and reconstruction strategies to prevent the recurrence of resource-driven degradation. This study demonstrates that the Sunut Reserved Forest underwent catastrophic deforestation between 2023 and 2026, driven primarily by direct tree removal during a period of governance breakdown. The rapidity and magnitude of forest depletion indicate a regime shift rather than incremental degradation. This case illustrates the broader principle that armed conflict can act as an accelerant of environmental collapse when institutional safeguards fail. Without rapid restoration and reinforcement of governance, the ecological and hydrological consequences may persist for decades.

5. Conclusion

This study provides robust, multi-method evidence of rapid and large-scale forest loss in the Sunut Reserved Forest between 2023 and 2026. Using high-resolution PlanetScope imagery, NDVI analysis, object-based classification, and non-parametric statistical approaches, the results demonstrated an 80.83% reduction in forest cover within three years, with a marked acceleration after 2025.

The integration of spectral indices and machine-learning classification, supported by independent validation and consistent temporal analysis, provides high confidence in the detected magnitude and spatial coherence of the change. Analysis of long-term climate data (2015–2025) indicated no significant rainfall or temperature anomalies, suggesting that climatic variability alone is unlikely to explain the observed vegetation decline. However, the potential influence of hydrological factors associated with the White Nile could not be evaluated and should be considered in future investigations. The results therefore point to a rapid transition from a predominantly forested landscape to a largely non-forest condition within a short time frame.

This study highlights the effectiveness of high-resolution satellite data combined with robust statistical methods for detecting and quantifying rapid land degradation in data-scarce and inaccessible environments worldwide. The methodological framework applied in this study offers a scalable approach for monitoring similar ecosystems under conditions of limited field access.

From a management perspective, the findings underscore the urgent need to prioritize the restoration and protection of urban riparian forests, particularly in regions affected by socio-political instability. However, ecological restoration alone is unlikely to be effective without concurrently strengthening environmental governance, enforcement mechanisms, and community-based management strategies.

From a monitoring perspective, future research should prioritize the integration of multi-sensor remote sensing approaches, particularly Synthetic Aperture Radar (SAR) data (e.g., Sentinel-1), which are not affected by cloud cover or atmospheric conditions. SAR can complement optical imagery by capturing vegetation structural changes and improving monitoring reliability under challenging conditions such as smoke or haze. Additionally, combining PlanetScope with Sentinel-2 time series data would enhance the temporal resolution and improve the detection of rapid land-use transitions.

Overall, this study demonstrates how rapid environmental change can be effectively quantified using integrated remote sensing approaches, providing critical evidence to support timely intervention, post-disturbance recovery planning, and sustainable ecosystem management in the futuer.

Funding

This research receives no funds.

CRediT authorship contribution statement

Abdalrahman Ahmed: Conceptualization, Data curation, Formal analysis, Methodology, Software, Validation, Writing – original draft, Writing – review & editing. **Abubakr Osman:** Writing – review & editing. **Kornel Czimber:** Supervision, Writing – review & editing.

Declaration of competing interest

The authors declare that they have no known competing financial interests or personal relationships that could have appeared to influence the work reported in this paper.

Data availability

Data will be made available on request.

References

Abdullahi, M.B., El-Naggar, A., Omar, M., Murtala, A.I., Lawal, M., Mosa, A., 2023. Land degradation, causes, implications and sustainable management in arid and semi arid regions: a case study of Egypt. Egypt. J. Soil Sci. 63 (4), 0. https://doi.org/10.21608/ejss.2023.230986.1647.

Ahmed, Kheiry, M.A., Mofadel Hassan, I.A., 2018. Impact of vegetation cover changes on gum Arabic production using remote sensing applications in Gedarif State, Sudan. Gum Arabic: Struct., Properties, Appl. Econ. 29–43. https://doi.org/10.1016/B978-0-12-812002-6.00004-X.

Ahmed, A., Rotich, B., Czimber, K., 2025a. Climate change as a double-edged sword: exploring the potential of environmental recovery to foster stability in Darfur, Sudan. Climate 13 (3), 63. https://doi.org/10.3390/CLI13030063, 2025, Vol. 13, Page 63.

Ahmed, A., Rotich, B., Kipkulei, H.K., Lameck, A.S., Gallai, B., Czimber, K., 2025b. Vegetation dynamics and climate variability in conflict zones: a case study of sortony internally displaced camp, Darfur, Sudan. Land. (Basel) 14 (8), 1680. https://doi.org/10.3390/LAND14081680, 2025, Vol. 14, Page 1680.

Aldwaik, S.Z., Pontius, R.G., 2012. Intensity analysis to unify measurements of size and stationarity of land changes by interval, category, and transition. Landsc. Urban. Plan. 106 (1), 103–114. https://doi.org/10.1016/j.landurbplan.2012.02.010.

Atwal, K.S., Pfoser, D., Rothbart, D., 2026. Near–Real-Time Conflict-Related Fire Detection Using Unsupervised Deep Learning and Satellite Imagery. https://arxiv.org/pdf/2512.07925v1.

Balthazar, V., Vanacker, V., Molina, A., Lambin, E.F., 2015. Impacts of forest cover change on ecosystem services in high Andean mountains. Ecol. Indic. 48, 63–75. https://doi.org/10.1016/j.ecolind.2014.07.043.

Basheer, M., Elagib, N.A., 2024. Armed conflict as a catalyst for increasing flood risk. Environ. Res. Lett. 19 (10), 104034. https://doi.org/10.1088/1748-9326/ad6fb6.

Baumann, M., Science, T. K.-J. of land use, & 2016, undefined, 2016. The impacts of warfare and armed conflict on land systems. Taylor & Francis 11 (6), 672–688. https://doi.org/10.1080/1747423X.2016.1241317.

Baumann, M., Kuemmerle, T., Elbakidze, M., Ozdogan, M., Radeloff, V.C., Keuler, N.S., Prishchepov, A.V., Kruhlov, I., Hostert, P., 2011. Patterns and drivers of post-socialist farmland abandonment in Western Ukraine. Land. Use Policy 28 (3), 552–562. https://doi.org/10.1016/j.landusepol.2010.11.003.

Baumann, M., Kuemmerle, T., 2016. The impacts of warfare and armed conflict on land systems. J. Land Use Sci. 11 (6), 672–688. https://doi.org/10.1080/1747423X.2016.1241317.

Biswas, N., & Islam, K.S. (2025). Assessing the impact of land use and land cover changes on land surface temperature dynamics in the coastal region of Bangladesh: a comprehensive analysis using deep learning techniques AHP integration. https://doi.org/10.21203/rs.3.rs-6800634/v1.

Bruijnzeel, L.A., 2004. Hydrological functions of tropical forests: not seeing the soil for the trees? Agric. Ecosyst. Environ. 104 (1), 185–228. https://doi.org/10.1016/j.agee.2004.01.015.

Cechim Junior, C., Araki, H., de Campos Macedo, R., 2023. Object-based image analysis (obia) and machine learning (ml) applied to tropical forest mapping using sentinel-2. Taylor & Francis 49 (1), 2259504. https://doi.org/10.1080/07038992.2023.2259504.

CEOBS, 2025a. The environmental costs of the war in Sudan - CEOBS. https://ceobs.org/the-environmental-costs-of-the-war-in-sudan/.

CEOBS, 2025b. The environmental costs of the war in Sudan - CEOBS. https://ceobs.org/the-environmental-costs-of-the-war-in-sudan/.

Chaves, M.E.D., Picoli, M.C.A., Sanches, I.D., 2020. Recent applications of Landsat 8/OLI and Sentinel-2/MSI for land use and land cover mapping: a systematic review. Rem. Sens. (Basel) 12 (18), 3062. https://doi.org/10.3390/RS12183062, 2020, Vol. 12, Page 3062.

Clerici, N., Armenteras, D., Kareiva, P., Botero, R., Ramírez-Delgado, J.P., Forero-Medina, G., Ochoa, J., Pedraza, C., Schneider, L., Lora, C., Gómez, C., Linares, M., Hirashiki, C., Biggs, D., 2020. Deforestation in Colombian protected areas increased during post-conflict periods. Sci. Rep. 10 (1), 4971. https://doi.org/10.1038/s41598-020-61861-y, 2020 10:1-.

Congalton, R., Green, K., 2009. Assessing the Accuracy of Remotely Sensed Data Principles and Practices, 3rd Edition.

Daur, N., Adam, Y.O., Pretzsch, J., 2016. A historical political ecology of forest access and use in Sudan: implications for sustainable rural livelihoods. Land. Use Policy 58 (4), 95–101. https://doi.org/10.1016/j.landusepol.2016.06.016.

Davis, K.F., Koo, H.I., Dell'Angelo, J., D'Odorico, P., Estes, L., Kehoe, L.J., Kharratzadeh, M., Kuemmerle, T., Machava, D., Pais, A., de, J.R., Ribeiro, N., Rulli, M.C., Tatlhego, M., 2020. Tropical forest loss enhanced by large-scale land acquisitions. Nat. Geosci. 13 (7), 482–488. https://doi.org/10.1038/s41561-020-0592-3, 2020 13:7.

Duffy, R., 2006. The potential and pitfalls of global environmental governance: the politics of transfrontier conservation areas in Southern Africa. Polit. Geogr. 25 (1), 89–112. https://doi.org/10.1016/j.polgeo.2005.08.001.

Eklund, L., Degerald, M., Brandt, M., Prishchepov, A.V., Pilesjö, P., 2017. How conflict affects land use: agricultural activity in areas seized by the Islamic State. Environ. Res. Lett. 12 (5), 054004. https://doi.org/10.1088/1748-9326/aa673a.

Ellison, D., Morris, C.E., Locatelli, B., Sheil, D., Cohen, J., Murdiyarso, D., Gutierrez, V., Noordwijk, M.van, Creed, I.F., Pokorny, J., Gaveau, D., Spracklen, D.V., Tobella, A. B., Ilstedt, U., Teuling, A.J., Gebrehiwot, S.G., Sands, D.C., Muys, B., Verbist, B., Sullivan, C.A., 2017. Trees, forests and water: cool insights for a hot world. Global Environmental Change 43 (6273), 51–61. https://doi.org/10.1016/j.gloenvcha.2017.01.002.

Eltayeb, H., Idris, E., Adam, A., T. E.- A. J. of, 2012, undefined, 2012. A forest in a city Biodiversity at Sunut forest, Khartoum, Sudan. Journals. Ekb. EgH Eltayeb, EIdris, AAdam, T Ezaldeen, D Hamedegyptian Academic Journal of Biological Sciences, B. Zoology, 2012•Journals.Ekb.Eg. https://journals.ekb.eg/article_14301_2cf6f2e9f89e845c9f3e80ce24483ae4.pdf.

Elzubair, A.E.M., Fadual, S.M., Elkarium, M.A., 2024. Participatory forest management as an approach to forest management and conservation: a case study of Al-Dalu and Al-Tomama Natural Forests in Sharg Al-Neel Locality, Khartoum State, Sudan. Int. For. Rev. 26 (4), 444–453. https://doi.org/10.1505/146554824839334678.

Fahrig, L., 2003. Effects of habitat fragmentation on biodiversity. Annu Rev. Ecol. Evol. Syst. 34, 487–515. https://doi.org/10.1146/annurev.ecolsys.34.011802.132419. Volume 34, 2003.

FAO, 2020. Global Forest Resources Assessment – Sudan Country Report - Google Search. FAO. (2020). https://www.google.com/search?q=FAO.+%282020%29.+Global+Forest+Resources+Assessment+%E2%80%93+Sudan+Country+Report&sca_esv=ad175a4a610f2e0b&rlz=1C1GCEA_enHU1096HU1096&sxsrf=ANbL-n40fR35drDyA1ScagXUdQCi2PTvXg%3A1772653934739&ei=bo2oadzpLPKcseMPv_2u0QQ&biw=1536&bih=742&ved=0ahUKEwjc2NvAgoeTAxVyTmwGHb–K0oQ4dUDCBE&uact=5&oq=FAO.+%282020%29.+Global+Forest+Resources+Assessment+%E2%80%93+Sudan+Country+Report&gs_lp=Egxnd3Mtd2l6LXNlcnAiSEZBTy4gKDIwMjApLiBHbG9iYWwgRm9yZXN0IFJlc291cmNlcyBBc3Nlc3NtZW50IOKAkyBTdWRhbiBDb3VudHJ5IFJlcG9ydEi1CFAAWABwAHgAkAEAmAGRAaABkQGqAQMwLjG4AQPIAQD4AQL4AQGYAgCgAgCYAwCSBwCgB3-yBwC4BwDCBwDIBwCACAA&sclient=gws-wiz-serp.

Foley, J.A., DeFries, R., Asner, G.P., Barford, C., Bonan, G., Carpenter, S.R., Chapin, F.S., Coe, M.T., Daily, G.C., Gibbs, H.K., Helkowski, J.H., Holloway, T., Howard, E.A., Kucharik, C.J., Monfreda, C., Patz, J.A., Prentice, I.C., Ramankutty, N., Snyder, P.K., 2005. Global consequences of land use. Science (1979) 309 (5734), 570–574. https://doi.org/10.1126/science.1111772. Number.

France 24. (2026). Sudan's historic acacia forest devastated as war fuels logging. https://www.france24.com/en/live-news/20260219-sudan-s-historic-acacia-forest-devastated-as-war-fuels-logging.

Gashaw, T., Tulu, T., Argaw, M., Worqlul, A.W., Tolessa, T., Kindu, M., 2018. Estimating the impacts of land use/land cover changes on ecosystem service values: the case of the Andassa watershed in the Upper Blue Nile basin of Ethiopia. Ecosyst. Serv. 31, 219–228. https://doi.org/10.1016/J.ECOSER.2018.05.001.

Gaynor, K.M., Fiorella, K.J., Gregory, G.H., Kurz, D.J., Seto, K.L., Withey, L.S., Brashares, J.S., 2016. War and wildlife: linking armed conflict to conservation. Front. Ecol. Environ. 14 (10), 533–542. https://doi.org/10.1002/fee.1433.

Geist, H.J., Lambin, E.F., 2002. Proximate causes and underlying driving forces of tropical deforestation. Bioscience 52 (2), 143. https://doi.org/10.1641/0006-3568(2002)052[0143:PCAUDF]2.0.CO;2.

Gorsevski, V., Kasischke, E., Dempewolf, J., Loboda, T., Grossmann, F., 2012. Analysis of the impacts of armed conflict on the Eastern Afromontane forest region on the South Sudan - Uganda border using multitemporal landsat imagery. Rem. Sens. Environ. 118, 10–20. https://doi.org/10.1016/j.rse.2011.10.023.

Guo, J., Gong, P., Dronova, I., Zhu, Z., 2022. Forest cover change in China from 2000 to 2016. Int. J. Rem. Sens. 43 (2), 593–606. https://doi.org/10.1080/01431161.2021.2022804.

Han, Y., Oh, J., 2018. Automated geo/Co-registration of multi-temporal very-high-resolution imagery. Sensors 18 (5), 1599. https://doi.org/10.3390/s18051599, 2018, Vol. 18.

Hassan, R., Hertzler, G., Benhin, J.K.A., 2009. Depletion of forest resources in Sudan: intervention options for optimal control. Energy Policy 37 (4), 1195–1203. https://doi.org/10.1016/j.enpol.2008.10.049.

Hosonuma, N., Herold, M., De Sy, V., De Fries, R.S., Brockhaus, M., Verchot, L., Angelsen, A., Romijn, E., 2012. An assessment of deforestation and forest degradation drivers in developing countries. Environ. Res. Lett. 7 (4), 044009. https://doi.org/10.1088/1748-9326/7/4/044009.

Huang, Q., Jin, G., Xiong, X., Ye, H., Xie, Y., 2023. Monitoring urban change in conflict from the perspective of optical and SAR satellites: the case of Mariupol, a City in the conflict between RUS and UKR. Rem. Sens. (Basel) 15 (12), 3096. https://doi.org/10.3390/RS15123096, 2023, Vol. 15, Page 3096.

Khan, M., Chen, R., 2025. Assessing the impact of land use and land cover change on environmental parameters in Khyber Pakhtunkhwa, Pakistan: a comprehensive study and future projections. Rem. Sens. (Basel) 17 (1), 170. https://doi.org/10.3390/rs17010170, 2025, Vol. 17.

Kranz, O., Sachs, A., Lang, S., 2015. Assessment of environmental changes induced by internally displaced person (IDP) camps in the Darfur region, Sudan, based on multitemporal MODIS data. Int. J. Rem. Sens. 36 (1), 190–210. https://doi.org/10.1080/01431161.2014.999386.

Krieger, D., 2001. Economic Value of Forest Ecosystem Services: a Review. http://www.sierraforestlegacy.org/Resources/Conservation/FireForestEcology/ForestEconomics/Economics-Krieger01.pdf.

Lambin, E.F., Turner, B.L., Geist, H.J., Agbola, S.B., Angelsen, A., Bruce, J.W., Coomes, O.T., Dirzo, R., Fischer, G., Folke, C., George, P.S., Homewood, K., Imbernon, J., Leemans, R., Li, X., Moran, E.F., Mortimore, M., Ramakrishnan, P.S., Richards, J.F., Xu, J., 2001. The causes of land-use and land-cover change: moving beyond the myths. Glob. Environ. Change 11 (4), 261–269. https://doi.org/10.1016/S0959-3780(01)00007-3.

Mahgoub, E.A.A., Khairy, A., Osman, S., Haga, M.B., Osman, S.H.M., Abbu Hassan, A.M., Kamal, H., Babiker, A., 2024. War and education: the attacks on medical schools amidst ongoing armed conflict, Sudan 2023. Confl. Health 18 (1), 23. https://doi.org/10.1186/s13031-024-00584-7, 2024 18:1-.

Meaza, H., Hishe, S., Gebrehiwot, M., 2024. Effects of war and siege on farmers' Livelihoods in Tigray, Ethiopia: lessons for conflict-vulnerable areas. Hum. Ecol. 52 (4), 877–890. https://doi.org/10.1007/s10745-024-00534-0, 2024 52:4.

Ming, D., Li, J., Wang, J., Zhang, M., 2015. Scale parameter selection by spatial statistics for GeOBIA: using mean-shift based multi-scale segmentation as an example. ISPRS J. Photogramm. Rem. Sens. 106, 28–41. https://doi.org/10.1016/j.isprsjprs.2015.04.010.

Mir, Y.H., Mir, S., Ganie, M.A., Bhat, J.A., Shah, A.M., Mushtaq, M., & Irshad, I. (2025). Overview of land use and land cover change and its impacts on natural resources. 101–130. https://doi.org/10.1007/978-981-96-2413-3_5.

Mishkin, M., Navarrete Pacheco, J.A., 2022. Rapid assessment remote sensing of forest cover change to inform forest management: case of the monarch reserve. Ecol. Indic. 137, 108729. https://doi.org/10.1016/j.ecolind.2022.108729.

Musa, F.I., Adlan Abdelkareem, O.E., Ali Abdelrhman, H., Sahoo, U.K., Eltahir, M.E.S., Mohamed, A.A.A., Fragallah, S.A.D., Elamin, H.M.A., 2025. Value chain of Grewia tenax fruits, and its contribution to different actors in Sheikan Locality, North Kordofan State, Sudan. Journal of Sustain. For. 44 (10), 1163–1180. https://doi.org/10.1080/10549811.2025.2574017.

Nardi, M.A., Runnström, M., 2024. Environmental change in conflict and post-conflict northern Uganda: a geographical analysis to understand prospects for sustainable peace and development in the. Journals.Sagepub.Com 33 (4), 698–729. https://doi.org/10.1177/10704965241258082.

Nedd, R., Light, K., Owens, M., James, N., Johnson, E., Anandhi, A., 2021. A synthesis of land use/land cover studies: definitions, classification systems, meta-studies, challenges and knowledge gaps on a global landscape. Land. (Basel) 10 (9), 994. https://doi.org/10.3390/LAND10090994, 2021, Vol. 10, Page 994.

Nicholson, S.E., Acs, F., Bordi, I., Wang, D.-Y., 2013. The West African Sahel: a review of recent studies on the rainfall regime and its interannual variability. Wiley Online Library 2013, 1–32. https://doi.org/10.1155/2013/453521.

Nicholson, S.E., Funk, C., Fink, A.H., 2018. Rainfall over the African continent from the 19th through the 21st century. Glob. Planet. Change 165, 114–127. https://doi.org/10.1016/J.GLOPLACHA.2017.12.014.

Ordway, E.M., 2015. Political shifts and changing forests: effects of armed conflict on forest conservation in Rwanda. Glob. Ecol. Conserv. 3, 448–460. https://doi.org/10.1016/j.gecco.2015.01.013.

Osman, K.T., 2014. Soil degradation, conservation and remediation. Soil Degrad., Conserv. Remediat., 9789400775909 https://doi.org/10.1007/978-94-007-7590-9.

Osman, M.M., Sevinc, H., 2019. Adaptation of climate-responsive building design strategies and resilience to climate change in the hot/arid region of Khartoum, Sudan. Sustain. Cities. Soc. 47 (1), 101429. https://doi.org/10.1016/j.scs.2019.101429.

Pettorelli, N., Vik, J.O., Mysterud, A., Gaillard, J.M., Tucker, C.J., Stenseth, N.C., 2005. Using the satellite-derived NDVI to assess ecological responses to environmental change. Trends Ecol. Evol. 20 (9), 503–510. https://doi.org/10.1016/J.TREE.2005.05.011/ASSET/F0804C7E-DDE9-4A1A-A562-F0867451416E/MAIN.ASSETS/GR1.JPG.

Reij, C., Tappan, G., M. S.-P. htt p://w ww.ifpri.org/sites, & 2009, undefined, 2009. Agro-environmental transformation in the Sahel: another kind of" Green Revolution". Desertcultivation.Org. https://books.google.com/books?hl=en&lr=&id=mmmkf5tsdT0C&oi=fnd&pg=PP5&dq=Agroenvironmental+transformation+in+the+Sahel&ots=JoMY3Ly2pN&sig=oii9eYlkNh6YbAJb3S22fUPZx1o.

Rudel, T.K., Defries, R., Asner, G.P., Laurance, W.F., 2009. Changing drivers of deforestation and new opportunities for conservation. Conserv. Biol. 23 (6), 1396–1405. https://doi.org/10.1111/J.1523-1739.2009.01332.X;PAGE:STRING:ARTICLE/CHAPTER.

Salah, O., Sciences, E. I.-A. J. of B., B, undefined, & 2013, undefined, 2013. A note on the bird diversity at two sites in Khartoum, Sudan. Eajbsz.Journals.Ekb.EgO Salah, E Idrisegyptian Academic Journal of Biological Sciences, B. Zoology, 2013•eajbsz.Journals.Ekb.Eg. https://eajbsz.journals.ekb.eg/article_13505_165b53b1829fed842fe0a813be6f1f07.pdf.

Sulieman, H.M., 2018. Exploring the spatio-temporal processes of communal rangeland grabbing in Sudan. Pastoralism 8 (1), 14. https://doi.org/10.1186/s13570-018-0117-5, 2018 8:1.

Sulieman, H.M., Ahmed, A.G.M., 2013. Monitoring changes in pastoral resources in eastern Sudan: a synthesis of remote sensing and local knowledge. Pastoralism 3 (1), 22. https://doi.org/10.1186/2041-7136-3-22.

Townshend, J.R., Masek, J.G., Huang, C., Vermote, E.F., Gao, F., Channan, S., Sexton, J.O., Feng, M., Narasimhan, R., Kim, D., Song, K., Song, D., Song, X.P., Noojipady, P., Tan, B., Hansen, M.C., Li, M., Wolfe, R.E., 2012. Global characterization and monitoring of forest cover using Landsat data: opportunities and challenges. Int. J. Digit. Earth. 5 (5), 373–397. https://doi.org/10.1080/17538947.2012.713190.

Tucker, C.J., 1979. Red and photographic infrared linear combinations for monitoring vegetation. Rem. Sens. Environ. 8 (2), 127–150. https://doi.org/10.1016/0034-4257(79)90013-0.

UNEP, 2007. UNEP. (2007). Sudan Post-Conflict Environmental Assessment. - Google Search. https://www.google.com/search?q=UNEP.+(2007).+Sudan+Post-Conflict+Environmental+Assessment.&rlz=1C1GCEA_enHU1096HU1096&oq=UNEP.+(2007).+Sudan+Post-Conflict+Environmental+Assessment.&gs_lcrp=EgZjaHJvbWUyBggAEEUYOTIGCAEQIxgnMgoIAhAAGAoYFhgeMgcIAxAAGO8FMgcIBBAAGO8FMgoIBRAAGIAEGKIEMgcIBhAAGO8FMgYIBxBFGDzSAQc4NjVqMGo0qAICsAIB8QWXJIqs_z10_A&sourceid=chrome&ie=UTF-8.

UNEP, 2025. Can This Iconic Sudanese Forest Come Back from the Brink? https://www.unep.org/news-and-stories/story/can-iconic-sudanese-forest-come-back-brink.

Van Uhm, D.P., Tjoonk, M.M., Bakole, E.Y., 2022. Organized forest crimes: charcoal and timber trade in the Democratic Republic of the Congo. The Private Sector and Organized Crime: Criminal Entrepreneurship, Illicit Profits, and Private Sector Security Governance, pp. 150–162. https://doi.org/10.4324/9781003198635-11.

Vanonckelen, S., Van Rompaey, A., 2015. Spatiotemporal analysis of the controlling factors of forest cover change in the Romanian Carpathian Mountains. Mt. Res. Dev. 35 (4), 338–350. https://doi.org/10.1659/MRD-JOURNAL-D-15-00014.

Venter, Z.S., Scott, S.L., Desmet, P.G., Hoffman, M.T., 2020. Application of Landsat-derived vegetation trends over South Africa: potential for monitoring land degradation and restoration. Ecol. Indic. 113, 106206. https://doi.org/10.1016/j.ecolind.2020.106206.

Winkler, K., Fuchs, R., Rounsevell, M., Herold, M., 2021. Global land use changes are four times greater than previously estimated. Nat. Commun. 12 (1). https://doi.org/10.1038/s41467-021-22702-2.

Yasin, E.H.E., Siddig, A.A.H., Deiab, E.E., Kornel, C., Hasoba, A., Osman, A., Yasin, E.H.E., Siddig, A.A.H., Deiab, E.E., Kornel, C., Hasoba, A., & Osman, A. (2023). Forest degradation in dryland ecosystems of Sudan: review of the causes, consequences, assessment methods, and potential solutions. https://doi.org/10.5772/intechopen.113222.

Yousif, L.A., Khatir, A.A., El-Hag, F.M., Abdelkarim, A.M., Adam, H.S., Wahab, A.A., Kurosaki, Y., Ali-Babiker, I.A., 2018. Rainfall variability and its implications for agricultural production in Gedarif State, Eastern Sudan. Afr. J. Agric. Res. 13 (31), 1577–1590. https://doi.org/10.5897/AJAR2018.13365.

Yusif, S., Cao, Y., Eissa, A., Elzaki, E., 2023. Economic assessment for the recreation value of Al-Sunut Forest Reserve in Khartoum State, Sudan. Sustainability 15 (24), 16779. https://doi.org/10.3390/su152416779, 2023, Vol. 15, Page 16779.

Yusif, S., Cao, Y., Eissa, A., Elzaki, E., Khalil, A., 2024. A measurement of perceptions of the Forest ecosystem among visitors to the AL-Sunut Forest Reserve in Khartoum, Sudan. Sustainability 16 (10), 4247. https://doi.org/10.3390/su16104247, 2024, Vol. 16.

Zheng, L., Zhang, J., Wang, Q., 2009. Mean-shift-based color segmentation of images containing green vegetation. Comput. Electron. Agric. 65 (1), 93–98. https://doi.org/10.1016/J.COMPAG.2008.08.002.

Zou, Z., Chen, K., Shi, Z., Guo, Y., Ye, J., 2023. Object detection in 20 years: a survey. Proc. IEEE 111 (3), 257–276. https://doi.org/10.1109/JPROC.2023.3238524.